

# Precessional Cycles and Their Influence on the North Pacific and North Atlantic Summer Anticyclones

DAMIANOS F. MANTSI, AMY C. CLEMENT, AND BEN KIRTMAN

*Rosenstiel School of Marine and Atmospheric Sciences, University of Miami, Miami, Florida*

ANTHONY J. BROCCOLI AND MICHAEL P. ERB

*Department of Environmental Sciences, Rutgers, The State University of New Jersey, New Brunswick, New Jersey*

(Manuscript received 13 June 2012, in final form 7 November 2012)

## ABSTRACT

The response of the Northern Hemisphere summer anticyclones to a change in the timing of perihelion is investigated using the GFDL Climate Model version 2.1 (CM2.1). The orbital forcing consists of changes in the seasonal cycle of the top-of-atmosphere insolation as the perihelion shifts from the Northern Hemisphere winter to the Northern Hemisphere summer solstice. The North Pacific summer anticyclone experiences a large strengthening as well as a northward and westward expansion. The North Atlantic subtropical high experiences a smaller change that consists of a slight westward expansion but little change in strength. Experiments with a primitive equation atmospheric model show that these changes represent the circulation response to changes in the diabatic heating, both local and remotely. The remote diabatic forcing is associated with changes in the Southeast Asian and African summer monsoons, and the local forcing is dominated by a combined effect of a change in low clouds and local precipitation.

## 1. Introduction

### *a. Modern theories on anticyclones*

The subtropical highs are among the most prominent features of the atmospheric general circulation, covering, during their seasonal peak, the entire subtropical-to-midlatitude basin. Even though Northern Hemisphere anticyclones are located over the oceans, they affect largely populated areas by regulating the summer hydrological cycle over the continent to the west (Zhou et al. 2009; Li et al. 2011). The Southern Hemisphere anticyclones peak during local winter and can be directly linked to the descending branch of the zonal mean Hadley circulation (Hoskins 1996; Seager et al. 2003; Nigam and Chan 2009). In contrast, the Northern Hemisphere anticyclones peak during local summer when the zonal mean Hadley circulation is at its minimum strength, implying that other processes have to be invoked to explain their maximum strength and extent.

Several studies regard the seasonality in the Northern Hemisphere summer anticyclonic circulation as the remote response to diabatic heating associated with monsoons. Hoskins (1996) showed, using a primitive equation model, that the adiabatic descent that takes place in the eastern part of the anticyclones is associated with the Rossby wave response to diabatic heating associated with the monsoons to the east of the anticyclones. Rodwell and Hoskins (2001) further suggested that heating associated with the adiabatic descent would have a net cooling effect by inhibiting latent heat release and increasing radiative cooling, thus strengthening this descent through a positive feedback (called local diabatic enhancement). They also suggested that the equatorward portion of each subtropical anticyclone can be viewed as a stationary Kelvin wave response (similar with the Gill model response to a heat source) to the monsoonal heating over the continent to the east. Idealized experiments with a linear quasigeostrophic model were also performed by Chen et al. (2001), highlighting the importance of the large-scale heat source over Asia to the development of the summer subtropical anticyclones over the North Pacific as well as the North Atlantic.

---

*Corresponding author address:* Damianos F. Mantsis, Department of Environmental Sciences, Rutgers University, 14 College Farm Rd., New Brunswick, NJ 08901.  
E-mail: dmantsis@envsci.rutgers.edu

Other studies attribute the peak of the Northern Hemisphere summer anticyclones to other effects besides monsoonal heating. Nigam and Chan (2009) suggested, based on the 40-yr European Centre for Medium-Range Weather Forecasts (ECMWF) Re-Analysis (ERA-40) dataset and idealized experiments with a primitive equation model, that roughly two-thirds of the seasonal strengthening of the Northern Hemisphere summer anticyclones can be attributed to the weakening and northward migration of the baroclinic activity, leaving a smaller contribution to monsoonal heating. The same study shows that this does not seem to be the case in the Southern Hemisphere since the baroclinic activity is located much closer to the poles, and it does not affect the seasonal cycle of the subtropical highs.

Furthermore, modeling studies (Miyasaka and Nakamura 2005, 2010) suggest that 70%–80% of the strength of the surface summer subtropical anticyclones in both hemispheres is directly forced by the local diabatic cooling–heating contrast in the lower troposphere between land and ocean. They showed that the intensification of the anticyclones is triggered by the late spring landmass warming, which takes place before the initiation of the monsoonal activity, and that the deep monsoonal heating plays a secondary role. Also, Wu and Liu (2003) argued, based on observational evidence, that a heating quadruplet pattern found over each subtropical continent and its adjacent oceans (dominated by sensible heating over the western continents, longwave radiative cooling over the eastern oceans, condensational heating over the eastern continents, and a combination of the last two over the western oceans) is associated with the summer anticyclones in each basin, implying that all diabatic processes contribute to the strength and extent of the subtropical highs.

The subtropical highs, in addition to covering a huge portion of the Northern Hemisphere, play an important role in the hydrological cycle of western North America and Asia by supplying moist warm air into the continents from the east. Zhou et al. (2009) showed that the summer subtropical high in the North Pacific has undergone a westward expansion over the second half of the twentieth century as a result of the observed Indian–western Pacific Ocean warming. According to their study, this IPO warming increases the convective activity in the western Pacific Ocean, which drives a stronger Walker circulation. This change in the Walker circulation is also associated with increased descending motion and reduced precipitation in the central-eastern tropical Pacific. Such an anomaly represents a negative heating anomaly and generates an anticyclonic response over the North Pacific that favors the westward expansion of the subtropical high. In addition, the strengthening of

the equatorial flank of the subtropical high is seen as a Kelvin wave response of the increased convective activity over the Indian/western Pacific region, as proposed by Rodwell and Hoskins (2001). Similar changes have also been shown for the North Atlantic anticyclone. Li et al. (2011) have shown that the North Atlantic summer anticyclone has undergone intensification and a westward expansion over the twentieth century as a result of anthropogenic forcing. According to the same study, these changes are expected to enhance under twenty-first-century warming, and this has the potential to increase the likelihood of both anomalously wet and dry summer conditions in the southeastern United States.

The mechanisms governing the interannual–decadal variability of the subtropical highs, as well as their response to external forcing from increasing greenhouse gases, are only beginning to be understood. Orbital forcing provides an opportunity to examine the sensitivity of the subtropical highs to external forcing, but it can also serve as a realistic and possible observable test for the theories that have been suggested to explain the strength and size of the anticyclones. Our study addresses the question of how the subtropical highs would change because of precession-induced changes in the insolation (Fig. 1).

#### *b. Monsoons and precessional cycle*

There is considerable previous work showing that the monsoons respond strongly to changes in the precessional cycle. Since monsoons are thought to be a primary driver of the subtropical highs, some background on this topic is relevant for understanding the complete atmospheric circulation to precessional forcing. The most illustrative example of orbital influence on the monsoons is the East Asian summer monsoon (EASM). Measurements of high-resolution oxygen isotope ( $\delta^{18}\text{O}$ ) profiles of stalagmites extracted from three different caves from southeast China (Wang et al. 2008) show that the EASM responded almost linearly to Northern Hemisphere summer insolation during the last 224 kyr. According to these proxies, the EASM was stronger when Northern Hemisphere summer insolation was increased as a result of the precessional forcing. Similar proxies from caves in Oman (Fleitmann et al. 2006) reveal that the Indian summer monsoon varied in phase with the EASM and the Northern Hemisphere summer insolation during the late mid-Holocene.

Another example is the hydrological cycle from tropical Africa, which also carries a pure precessional signal. Proxy records of lake and deep sea sediments from Africa show that, during the late Pleistocene (its last 200 kyr), the African summer monsoon on both sides of the equator was in phase with local summer

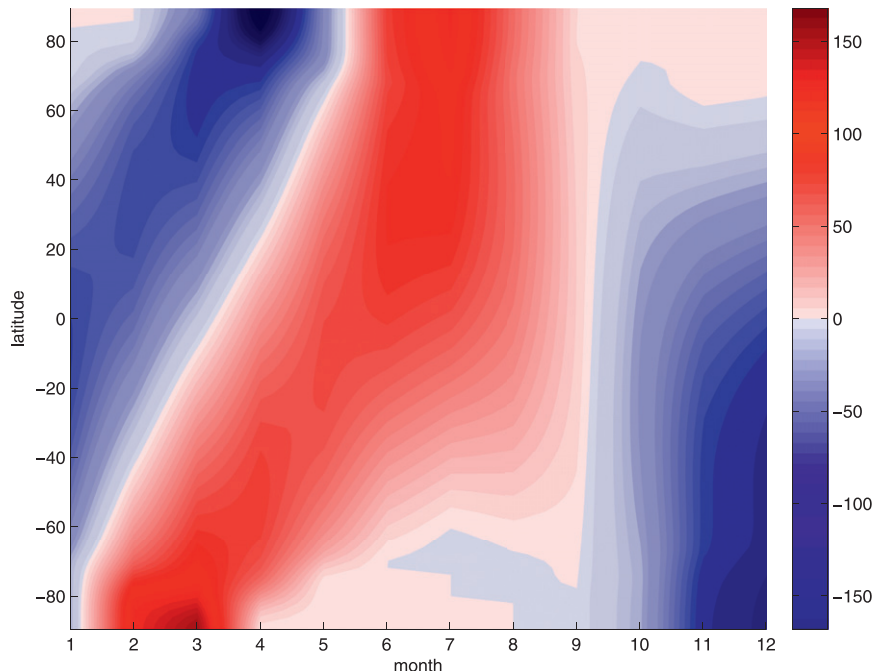


FIG. 1. Changes (SSOL – WSOL) in the seasonal cycle of the TOA insolation ( $\text{W m}^{-2}$ ).

insolation, which is dominated at low latitudes by Earth's precession (Partridge et al. 1997). Furthermore, fossilized pollen-based reconstructions of 6 kyr Before Present (BP) vegetation in northern Africa show that the size of the Saharan Desert was reduced considerably compared to its modern size, with steppe vegetation supported in its southern parts (Jolly et al. 1998; Wu et al. 2007; Lezine et al. 2011). Another observation of the same study, that the tropical rain forests of today's Cameroon could have been replaced by tropical deciduous forests in 6 kyr BP, supports the hypothesis that the monsoons of northern Africa were stronger during that time period, when Northern Hemisphere summer insolation was increased as a result of changes in precession.

It should be noted, though, that precipitation proxies also present some limitations. This is because the precessional variability of proxies also depends on processes that do not always reflect changes in local precipitation. For instance, it has been found that advection of moisture, traced from the Indian or Pacific Oceans (that have a different  $\delta^{18}\text{O}$  isotope signature) into southeastern Asia, can affect the variability of  $\delta^{18}\text{O}$  from local caves (LeGrande and Schmidt 2009; Pausata et al. 2011). This means that any precession-induced changes in moisture transport or the evaporation over the ocean regions can transmit the precessional signal to the variability of  $\delta^{18}\text{O}$  in caves, and therefore, the interpretation of such proxies should be done with caution.

The dramatic changes in the tropical hydrological cycle as a response to changes in Earth's precession, seen in the proxy record, are also supported by modeling studies. Early climate simulations showed that precession-induced increases in the summer insolation 9 kyr BP are associated with increased precipitation in the Asian summer monsoon (Kutzbach 1981; Prell and Kutzbach 1992). Furthermore, Kutzbach and Liu (1997) showed that precession-induced increases in summer insolation during the mid-Holocene (6 kyr BP) can reduce the meridional temperature gradient in the tropical Atlantic and shift the ITCZ northward, causing an increase in the northern African monsoon. Also, models from the Paleoclimate Modelling Intercomparison Project (PMIP) show that North African climate was wetter during the mid-Holocene compared to present day, supporting a greater lake area (Coe and Harrison 2002), and vegetation feedbacks play an important role in the northward shift of the African monsoon (Joussaume et al. 1999; Braconnot et al. 1999). Also, despite the fact that both African and Asian monsoons strengthen during the mid-Holocene, the Asian monsoon constrains the strengthening of the African monsoon through the subsidence it induces in the Mediterranean region (Marzin and Braconnot 2009).

Clement et al. (2004) showed, using an atmospheric-slab ocean model, that precessional forcing can have an effect on tropical precipitation that can be comparable to, or even overwhelm on a local scale, any remote

forcing from high-latitude ice sheets. Their study showed that while land precipitation in both hemispheres increases as a response to the precession-induced increase in local summer insolation, ocean precipitation behaves in the opposite way. Furthermore, mid-Holocene experiments documented in the PMIP2 archive also support a similar contrasting behavior in the tropical precipitation between land and ocean because of a change in precession (Braconnot et al. 2007a,b; Hsu et al. 2010).

The agreement between the simulated and recorded past monsoon changes implies that the anticyclones could have also changed in the past through the mechanisms outlined in section 1a. Our study addresses the question of how the subtropical highs would change because of precession-induced change in the insolation (Fig. 1). Is the subtropical high response driven by a monsoon–anticyclone interaction, as proposed by Hoskins (1996) and Rodwell and Hoskins (2001), or are the changes in the midlatitude baroclinic activity (Nigam and Chan 2009) and the local lower tropospheric land–ocean heating contrast more important (Miyasaka and Nakamura 2005, 2010)? This paper will address this question and will also explore the potential to test these ideas with paleoclimate proxies.

## 2. Model description and experimental design

For this study we use the Geophysical Fluid Dynamics Laboratory (GFDL) Climate Model version 2.1 (CM2.1). The experiment consists of two highly idealized simulations designed to isolate the effect of precession on climate. For this we will compare two runs with the longitude of the perihelion set to the Northern Hemisphere winter solstice (WSOL,  $90^\circ$ ) and the Northern Hemisphere summer solstice (SSOL,  $270^\circ$ ), but holding all nonorbital parameters (i.e., solar irradiance, greenhouse gas concentrations, and surface boundary conditions) to the same values as those used in preindustrial (i.e., 1860) simulations with CM2.1 (Delworth et al. 2006). To maximize the amplitude of the precessional cycle, we have run these simulations with an eccentricity of 0.0493, which is the maximum value during the last 600 kyr. The chosen eccentricity value is slightly larger than the maximum value that occurred during the last full glacial cycle (0.0440) and smaller than the maximum value that occurred during the past 5 Myr. Obliquity was also held constant at  $23.439^\circ$ .

Each of these simulations is initialized from year 1000 of a preindustrial run of CM2.1 with the altered orbital parameters imposed instantaneously. From there, each of these simulations is run for 400 years, which is sufficient for the surface and upper ocean to approach equilibrium.

The analysis focuses on the seasonal climate changes between the SSOL and WSOL simulation, and for this we use averages of the last 100 years of each simulation. Seasons were defined in the original runs based on the present-day calendar, with the autumnal equinox chosen as the fixed reference date (Joussaume and Braconnot 1997). However, because of the fact that the duration of each season changes as the longitude of the perihelion moves around Earth's orbit, a calendar conversion has been applied (Pollard and Reusch 2002), and the resulting monthly means resemble those defined based on angular months. It was tested that this calendar conversion did not affect the seasonal climate response significantly, and the initial uncorrected simulations were used instead.

We also use a primitive equation atmospheric model (AM) to study the mechanism responsible for the changes in the atmospheric circulation. The AM is a global, dry, hydrostatic model derived from Bourke (1974). Details of the model are also described in Vernekar et al. (1992), and the model has been used as a diagnostic model in Kirtman et al. (2001). It is nonlinear, spectral in the horizontal (R15 truncation), and uses finite differences in  $\sigma$  coordinates in the vertical. The horizontal resolution is  $7.5^\circ \times 4.5^\circ$ , and there are five levels in the vertical. The model is driven by Newtonian cooling and includes biharmonic dissipation in the temperature and momentum equations and Rayleigh damping in the vorticity and divergence equation.

The AM is used to test whether changes in the circulation, as documented by CM2.1, are related to changes in the diabatic heating ( $Q$ ). The diabatic heating in the CM2.1 is associated with five distinct physical processes: 1) absorption of shortwave radiation (SW), 2) absorption and emission of longwave radiation (LW), 3) vertical diffusion (VD) of heat induced by turbulence, 4) latent heat release associated with condensation of water vapor in stratus clouds (ST), and 5) latent heat release associated with condensation of water vapor in convective clouds (CC). CM2.1 resolves each physical process with a different parameterization scheme and computes the diabatic heating separately from the others. The sum of the diabatic heating corresponding to these five physical processes gives us the total diabatic heating.

Throughout this study, the AM is forced with the seasonal diabatic heating from CM2.1. For each AM run, the diabatic heating is held fixed to the average of the last 100 years of the CM2.1 runs. This is done separately for the WSOL and the SSOL case, and the difference in the response circulation is analyzed. This way changes in the circulation simulated by CM2.1 can be attributed to changes in the diabatic heating. Also, for

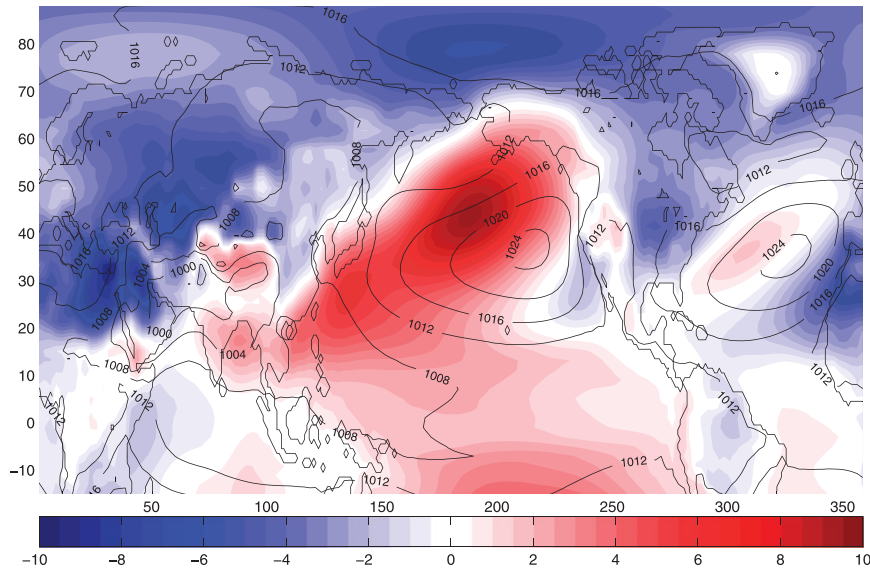


FIG. 2. The JJA seasonal means for sea level pressure. Contours represent the model's climatology and colors represent SSOL – WSOL anomalies (hPa).

the Newtonian cooling  $\tau^{-1}(T - T_{\text{CM2.1}})$ , which drives the atmospheric circulation in the AM, the temperature is relaxed toward the three-dimensional seasonal temperature of the CM2.1 ( $T_{\text{CM2.1}}$ ), acquired by averaging over the last 100 years of the CM2.1 run. Here the time scale parameter  $\tau$  represents the  $e$ -folding time it takes  $T$  to relax toward  $T_{\text{CM2.1}}$ . In order to isolate the effect of the diabatic heating variations on the circulation, the same 3D temperature profile, corresponding to the WSOL case, is used for all experiments. A scaling analysis showed that the prescribed  $Q$  is one order of magnitude larger compared to the Newtonian cooling. This is also the reason why the model results are not so sensitive to the choice of  $T_{\text{CM2.1}}$ , and similar results were acquired when the 3D temperature profile corresponding to the SSOL case was used instead.

Previous modeling studies of the subtropical anticyclones (Rodwell and Hoskins 2001; Chen et al. 2001; Miyasaka and Nakamura 2005, 2010) also use nonlinear primitive equation models, but they run the model only for 15–20 days. This is done in order to get the initial linear response and to avoid the effect from nonlinearity and baroclinicity, which is small in the initial stage of the simulations but grows and overwhelms the response after a few days. Such an approach is used because of the absence of solid nonlinear wave dynamics, and thus the existence of the anticyclones is explained in terms of linear wave dynamics. Here we focus on the fully nonlinear equilibrated response, which allows us to run longer simulations. It should be noted that the effect of nonlinear dynamics is found to be small in the Northern

Hemisphere summer circulation (see section 6 for more details). Each AM simulation is run for 3000 days. We neglect the spinup process (first 200 days), and the remaining 2800 days are averaged in order to isolate the equilibrated response from the internal variability of the AM.

### 3. Circulation response to the precessional forcing in the CM2.1

As the perihelion moves from WSOL to SSOL, the top-of-atmosphere (TOA) insolation undergoes changes both as a function of latitude as well as season. Figure 1 shows that the Northern Hemisphere experiences an intensification of the seasonal cycle due to an increase in insolation during boreal summer and a reduction of the insolation during boreal winter. In contrast, the Southern Hemisphere experiences a weakening of the seasonal cycle due to a reduction in insolation during austral summer and an increase in the insolation during austral winter. All diagnostics used in this study represent SSOL – WSOL anomalies.

For the Northern Hemisphere subtropical highs, which peak during boreal summer, the most notable feature is the increase in the maximum sea level pressure (SLP) of the North Pacific anticyclone by about 9 hPa (Fig. 2). The Pacific anticyclone also expands in almost all directions. The North Atlantic subtropical high shifts northwestward, but the anomalies are much smaller ( $\sim 2$  hPa). Also, a double-sided Student's  $t$  test showed that these changes are robust at the 5% significant level.

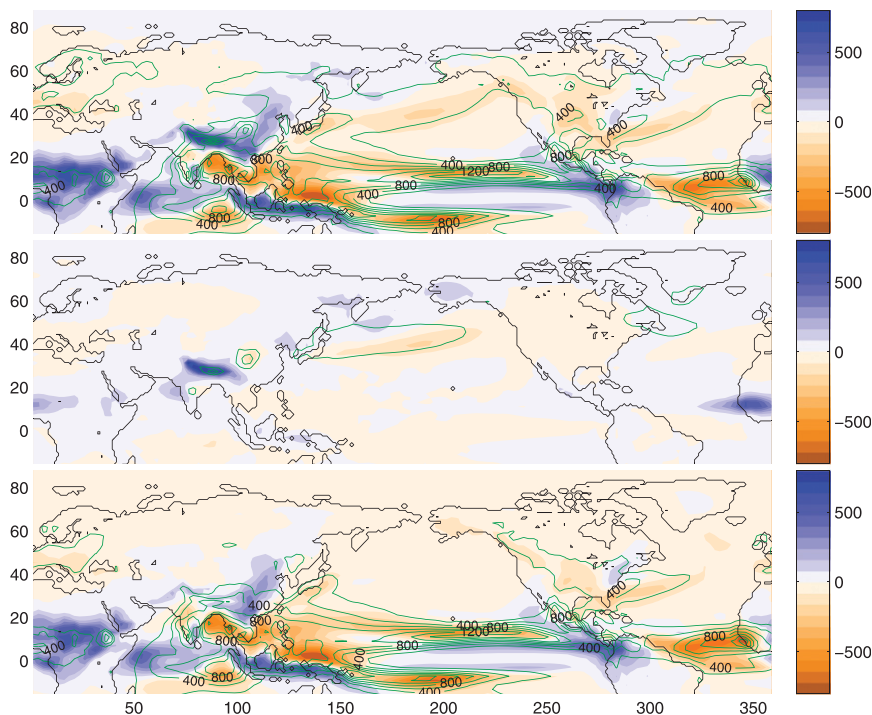


FIG. 3. The JJA seasonal means for (top) total, (middle) convective, and (bottom) large-scale precipitation. Contours represent the model's climatology and colors represent SSOL – WSOL anomalies ( $\text{mm month}^{-1}$ ).

Under climatological conditions, the tropical hydrological cycle is closely related to the annual cycle of TOA insolation, with maximum precipitation migrating from the southern to the northern tropics following local insolation maxima. Figure 3 shows the June–August (JJA) climatology, as well as the SSOL – WSOL anomalies of total, convective and large-scale precipitation, as simulated by CM2.1. During boreal summer (JJA), continental regions that normally get large amounts of precipitation like northern Africa, Indonesia, Southeast Asia, and central and northern South America experience an increase in convective precipitation as a result of increased local insolation due to precession. These results are consistent with the results of Clement et al. (2004), who used an atmospheric-slab ocean model to simulate the effect of precession on the tropical hydrological cycle. They also agree with the changes of the continental hydrological cycle, as documented by the available proxy record presented in the introduction (e.g., the variability of the Southeast Asian summer monsoons and the tropical African monsoon). In contrast with the precipitation changes that take place over land, over tropical oceans the simulated hydrological cycle behaves in the opposite way, with convective activity being suppressed during boreal summer. Also, the poleward expansion of the North Pacific

anticyclone is consistent with weaker summer baroclinic activity and a shift to the north, as seen by the reduced large-scale precipitation over the midlatitudes (Fig. 3, middle). A double-sided Student's  $t$  test showed that all precipitation changes are robust at the 5% significant level. To diagnose why the Northern Hemisphere anticyclones change, additional experiments with a simplified dynamical atmospheric model must be performed.

#### 4. Atmospheric model results

A set of experiments with a primitive equation atmospheric model was conducted in order to investigate the cause of the changes in the subtropical and midlatitude circulation. The AM was forced with the seasonal diabatic heating ( $Q$ ) taken from the output of the CM2.1 coupled model. In the first simulation with the AM, the model is forced with the JJA diabatic heating from the WSOL case ( $Q_{\text{WSOL}}$ ). This simulation represents the control run (CTRL). All simulations to follow (listed in Tables 1 and 2) will be compared with the CTRL run.

In the first experiment (called Land+Ocean), we force the AM with the JJA diabatic heating corresponding to the SSOL case ( $Q_{\text{SSOL}}$ ) and compare it to the CTRL run. Figure 4a shows that the AM can reproduce quite

TABLE 1. Experiments performed with the AM. The run that is compared with Run1 is forced with  $Q_{\text{WSOL}}$  globally for all experiments.

Experiment	Run1
Land+Ocean	$Q_{\text{SSOL}}$ global
Ocean	$Q_{\text{SSOL}}$ (Ocean) + $Q_{\text{WSOL}}$ (Land)
Land	$Q_{\text{SSOL}}$ (Land) + $Q_{\text{WSOL}}$ (Ocean)
NPac	$Q_{\text{SSOL}}$ (North Pacific) + $Q_{\text{WSOL}}$ (elsewhere)
NAtl	$Q_{\text{SSOL}}$ (North Atlantic) + $Q_{\text{WSOL}}$ (elsewhere)
NAtl+AtlITCZ	$Q_{\text{SSOL}}$ (North Atlantic and Atlantic ITCZ) + $Q_{\text{WSOL}}$ (elsewhere)
NPac+PacITCZ	$Q_{\text{SSOL}}$ (North Pacific and Pacific ITCZ) + $Q_{\text{WSOL}}$ (elsewhere)

accurately the SLP changes (of CM2.1) that occur in the Northern Hemisphere during local summer (JJA), though the AM slightly underestimates the strengthening of the subtropical high in the North Pacific. This implies that in the Northern Hemisphere, the changes in the atmospheric circulation are directly associated to the changes in the diabatic heating. These changes were also tested for statistical significance (using a double-sided Student's  $t$  test), and they were found to be significant at the 5% level.

The ability of the AM to simulate the Northern Hemisphere surface pressure response, which is driven by changes in the diabatic heating ( $Q$ ), raises an important question. Which region do the changes in  $Q$  come from? Is it ocean or land?

To answer this question, we perform another set of experiments. We force the AM by placing  $Q_{\text{WSOL}}$  in all regions except a certain region where we place  $Q_{\text{SSOL}}$ . By comparing this run with the CTRL run, we can attribute changes in the surface circulation to changes in  $Q$  that take place over that specific geographical region.

First, we force the atmospheric model with  $Q_{\text{SSOL}}$  over all ocean basins (experiment Ocean). This experiment reveals that the changes in the diabatic heating over the oceans are associated with anticyclonic anomalies (2–3 hPa) stationed over the subtropical to mid-latitude oceans (Fig. 4b). However, an experiment where we force the AM with  $Q_{\text{SSOL}}$  over land (experiment Land) shows that the anticyclonic circulation over the North Pacific seems to be remotely affected by the diabatic heating over land as well (Fig. 4c), something that does not happen in the North Atlantic. This suggests that the greater response in the anticyclonic circulation in the North Pacific compared to that in the North Atlantic is due to the remote response to heating over land. The calculation of the sum of the SLP responses to changes in  $Q$  over land and over the ocean (Fig. 4d) shows a remarkable similarity with the response to the change in diabatic heating globally (Fig. 4a). This means that the

TABLE 2. Experiments performed with the AM. The run that is compared with Run1 is forced with  $Q_{\text{WSOL}}$  globally for all experiments.

Experiment	Run1
NAfr	$Q_{\text{SSOL}}$ (North Africa) + $Q_{\text{WSOL}}$ (elsewhere)
SEAsia	$Q_{\text{SSOL}}$ (Southeast Asia) + $Q_{\text{WSOL}}$ (elsewhere)
SEAsia+NAfr	$Q_{\text{SSOL}}$ (North Africa and Southeast Asia) + $Q_{\text{WSOL}}$ (elsewhere)
Monsoon	$Q_{\text{SSOL}}$ (North Africa, Southeast Asia, Indonesian islands, and central and northern South America) + $Q_{\text{WSOL}}$ (elsewhere)
NAm	$Q_{\text{SSOL}}$ (North America) + $Q_{\text{WSOL}}$ (elsewhere)
LOHC1	Lower troposphere $Q_{\text{SSOL}}$ (North Pacific and North America) + $Q_{\text{WSOL}}$ (elsewhere)
LOHC2	Lower troposphere $Q_{\text{SSOL}}$ (LW over North Pacific and VD over North America) + total $Q_{\text{WSOL}}$ (elsewhere)

response is approximately linear, and such a result gives credibility to experiments where the AM is forced with change in the diabatic heating from an isolated geographical region.

Further experiments (NPac and NAtl) where the atmospheric model was forced with  $Q_{\text{SSOL}}$  over the North Pacific (between 18° and 68°N) and North Atlantic (between 18° and 75°N) separately reveal that local diabatic heating plays an important role for the anticyclonic anomalies over the northern basins (Figs. 5a,b). Where does this heating come from?

The area-weighted vertical profile of the change in the diabatic heating for the North Pacific and North Atlantic (Fig. 6) are similar. In both cases there is diabatic cooling of roughly equal magnitude that is almost constant throughout the troposphere. The fact that the  $Q$  anomalies are similar explains why the circulation response to the local forcing (Figs. 5a,b) is also similar in size and magnitude. One could argue that the diabatic cooling anomalies over the North Pacific and the North Atlantic are the result of the anticyclonic anomalies. However, this argument implies that the anticyclonic anomalies in the North Atlantic and North Pacific (corresponding to the original experiment) would need to have the same magnitude, which is not true. Instead, the anticyclonic anomaly over the North Atlantic is much smaller compared to the North Pacific. This means that the change in the local  $Q$  is not the result of the anticyclonic anomalies, but most likely represents a forcing for the anticyclonic anomalies.

Among the processes governing the diabatic cooling over the northern basins, the dominant one is the reduction of latent heat release from convective clouds (discussed later). This has maximum values in the lower-middle troposphere and is consistent with a stabilization

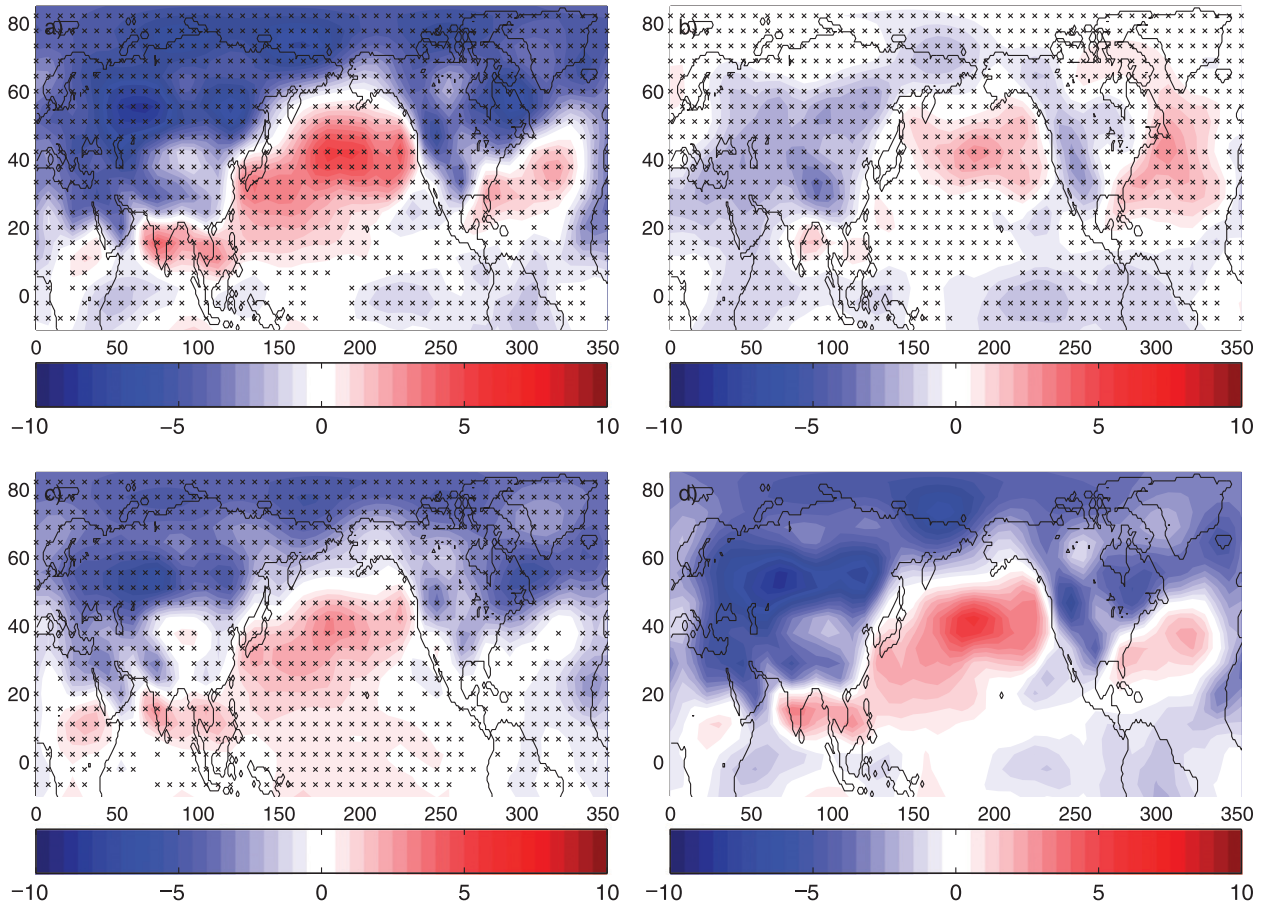


FIG. 4. Surface pressure response (hPa) of the AGCM to changes in the diabatic heating over (a) whole globe, (b) oceans only, (c) land only, and (d) sum of (b) and (c). Markers ( $\times$ ) show the statistical significance at the 95% level of significance.

of the atmosphere. An increase in the longwave radiative cooling also contributes to the tropospheric diabatic cooling and has maximum values in the lower, as well as the upper, troposphere. However, the diabatic cooling is partly compensated by the heating due to absorption of shortwave radiation throughout the troposphere and can be related to the imposed increase in the summer Northern Hemisphere insolation.

For experiments NPac and NAtl, the tropical part of the diabatic heating was kept unchanged, and they do not include the changes in the diabatic heating in the Pacific and Atlantic ITCZ (between  $17^{\circ}\text{S}$  and  $17^{\circ}\text{N}$ ) that experience large changes in precipitation (Fig. 3, middle) and latent heat (LH) release. An additional experiment (NPac+PacITCZ) that further includes the changes in the ITCZ part of the diabatic heating over the tropical Pacific reveals that the anticyclonic anomaly over the North Pacific has the same magnitude, but with a larger extent (Fig. 5c). In a similar experiment (NAtl+AtlITCZ) for the North Atlantic, the anticyclonic anomaly was stronger (by 1 hPa), indicating that

remote forcing from the Atlantic ITCZ could augment the North Atlantic circulation response that stems from the local forcing (Fig. 5d). A comparison of the change in the mean vertical diabatic heating profile between the tropical Atlantic and Pacific (between  $17^{\circ}\text{S}$  and  $17^{\circ}\text{N}$ ) showed that both regions experience a cooling, but for the tropical Atlantic, the cooling is 3 times larger (Fig. 6). This could explain why the change in the Atlantic ITCZ has a greater effect on the circulation response north of it compared to the Pacific ITCZ. In both regions the cooling is due to a reduction in convective precipitation and LH release. The smaller reduction in LH release in the tropical Pacific is because the central-east equatorial Pacific experiences an increase in convective activity that partly offsets the reduction in the rest of the region.

The fact that part of the changes in the surface circulation in the North Pacific is remotely forced by changes in the diabatic heating over land raises the question, which continental region contains the  $\Delta Q$  that is responsible for the anticyclonic anomaly over the North Pacific? Hoskins (1996) suggested that the Atlantic summer subtropical

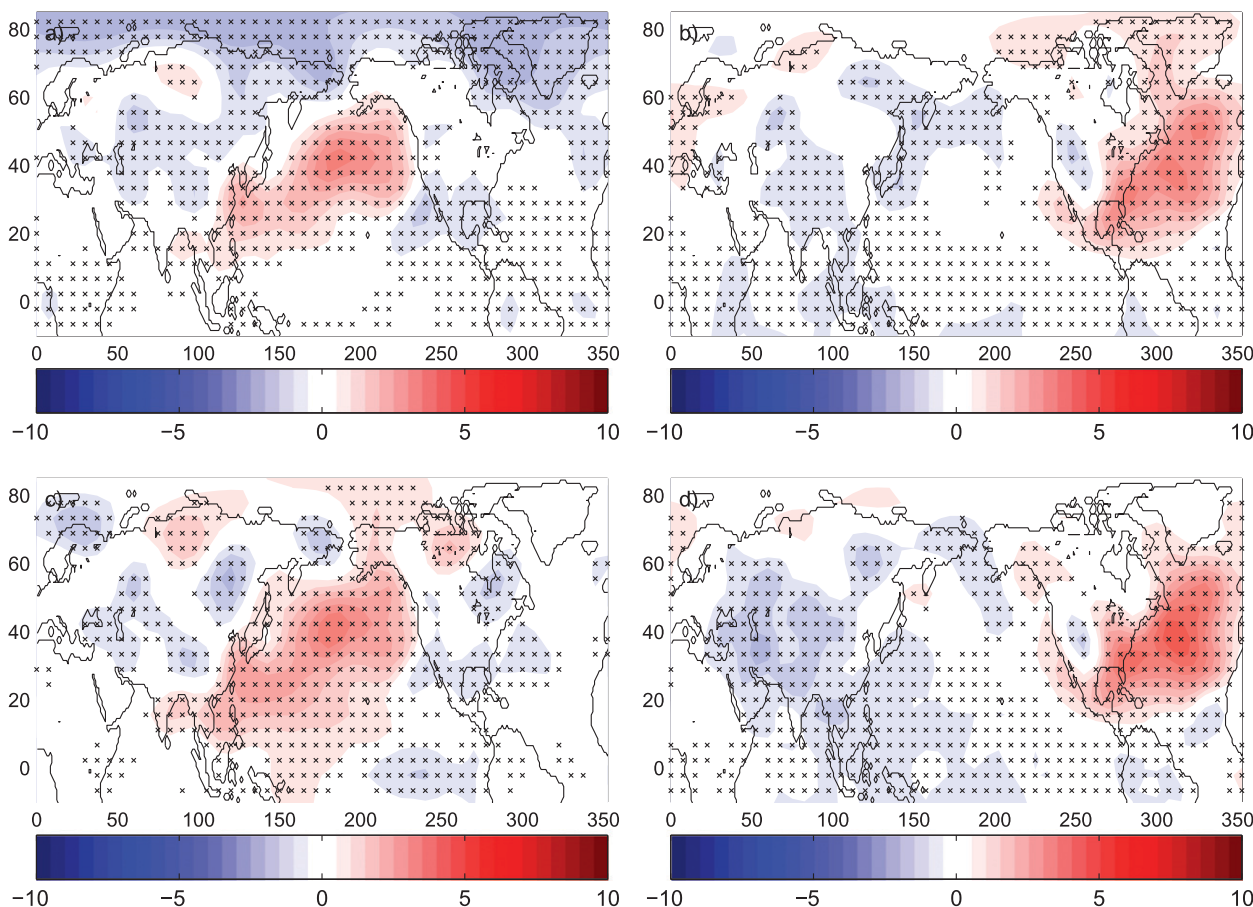


FIG. 5. Surface pressure response (hPa) to changes in the diabatic heating over (a) North Pacific, (b) North Atlantic, (c) North Pacific and Pacific ITCZ, and (d) North Atlantic and Atlantic ITCZ. Markers ( $\times$ ) show the statistical significance at the 95% level of significance.

anticyclone is partly forced by diabatic heating associated with the summer Asian monsoons. Therefore, the role of the strengthening in the continental monsoons is investigated. Figure 3 (middle panel) shows that the continental regions of Southeast Asia, northern tropical Africa, Indonesia, and northern South America experience large increases in precipitation, which are accompanied by large changes in  $Q$ .

An experiment (SEAsia) in which  $Q_{SSOL}$  was assigned over Southeast Asia (Fig. 7a) reveals that the response in circulation to these changes is a positive anticyclonic anomaly of magnitude  $\sim 1.5$  hPa over the North Pacific. Furthermore, adding the diabatic heating over North Africa (experiment SEAsia+NAfr) investigates the combined remote effect of both Southeast Asia and North African monsoon. The anticyclonic response over the North Pacific in this case is  $\sim 2.2$  hPa (Fig. 7b), which tells us that these two regions carry a large fraction of the remote response in the North Pacific. Another experiment (experiment Monsoon), where we included  $Q_{SSOL}$  over all continental tropical regions that experience an

increase in precipitation, gives a slightly stronger response ( $\sim 2.7$  hPa) over the North Pacific (Fig. 7c). However, experiments with the diabatic heating over the northern South America and Indonesia separately show that the changes in the monsoons over these regions have a very small remote influence on the North Pacific circulation (not shown). The vertical heating profile in Southeast Asia and North Africa, where we see the biggest increase in tropical precipitation over land, is dominated by the increase in LH heat release (Fig. 6).

Here it should be noted that a change in the heating over land that is not related to a change in monsoonal activity should not be underestimated. Experiment NAM shows that the increase in the heating over North America generates a positive anticyclonic anomaly in the northwest Pacific (Fig. 7d), contributing to the westward expansion of the Pacific anticyclone.

We also test the North Pacific circulation response to the change in the local lower tropospheric land–ocean heating contrast (LOHC). For this we perform an

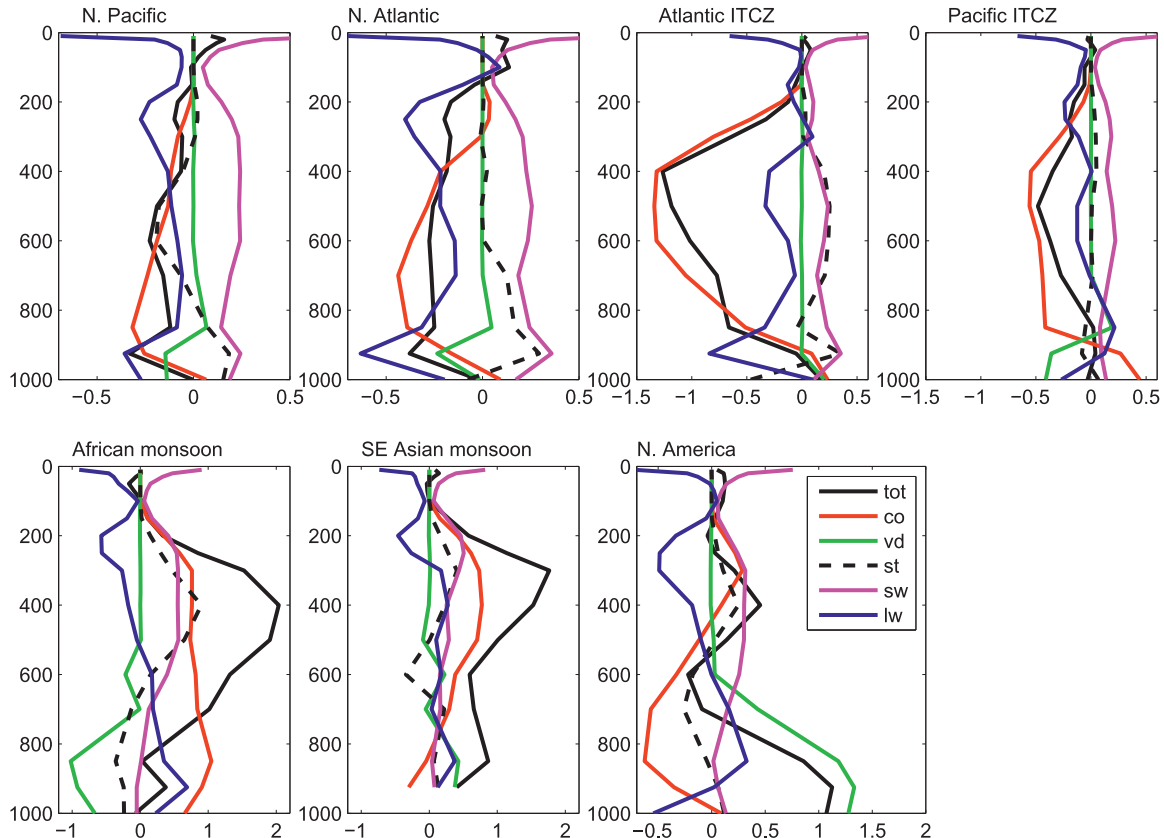


FIG. 6. Area-weighted average vertical changes in diabatic heating profile ( $10^{-5} \text{ K s}^{-1}$ ) for SW, VD, LW, ST, latent heat release in convective clouds (CO), and total heating (TOT) for the locations indicated. Notice that the scale is not the same for all regions.

experiment (LOHC1) where  $Q_{\text{SSOL}}$  is introduced in the lower troposphere (sigma levels 0.7 and 0.9) over North Pacific and North America and  $Q_{\text{WSOL}}$  is used at other levels and other regions. Figure 6 shows that the total diabatic heating anomalies (SSOL – WSOL) at the 0.9 sigma level constitute a strengthening of the land–ocean heating contrast between the North Pacific and North America. The response of the circulation in this case is a westward expansion as well as a small strengthening of the subtropical high (Fig. 7e). It should be noted that this strengthening of the land–ocean heating contrast in this region disappears at higher levels (0.7 sigma level), and a general cooling is observed. We also perform an experiment (LOHC2) where we introduce the longwave part of  $Q_{\text{SSOL}}$  over the North Pacific and  $Q_{\text{SSOL}}$  attributed to the vertical diffusion over North America. Again, for other regions, levels, and other physical processes, we use  $Q_{\text{WSOL}}$ . In this case, the lower tropospheric land–ocean heating contrast is stronger and better defined, and it extends higher (0.7 sigma level). The result is that, in this case, the North Pacific SLP response is stronger and again constitutes a westward expansion and a strengthening of the subtropical high (Fig. 7f).

## 5. $Q$ anomalies over the North Pacific and North Atlantic

Thus far, results show that part of the anticyclonic anomaly in the North Pacific is remotely forced by the change in the tropical monsoonal activity. However, the anticyclonic anomalies in both basins are also locally forced, as demonstrated by the AM experiments. Here we attempt to explain why the changes in the local diabatic heating take place.

First, let us look at how the precessional forcing affects the Northern Hemisphere JJA insolation. As JJA insolation increases, the surface temperature increases over the continents by several degrees, reaching as much as  $13^{\circ}\text{C}$  in the subtropical and midlatitude regions (Fig. 8, top left). These positive temperature anomalies are not constrained at the surface and extend to the upper troposphere. An inspection of the 700-hPa temperature anomalies (Fig. 8, top right) shows that the precession-induced temperature anomalies over the continents extend over the adjacent oceans. Despite the difference in the anticyclonic response in the two basins, the temperature anomalies over the North Pacific and North

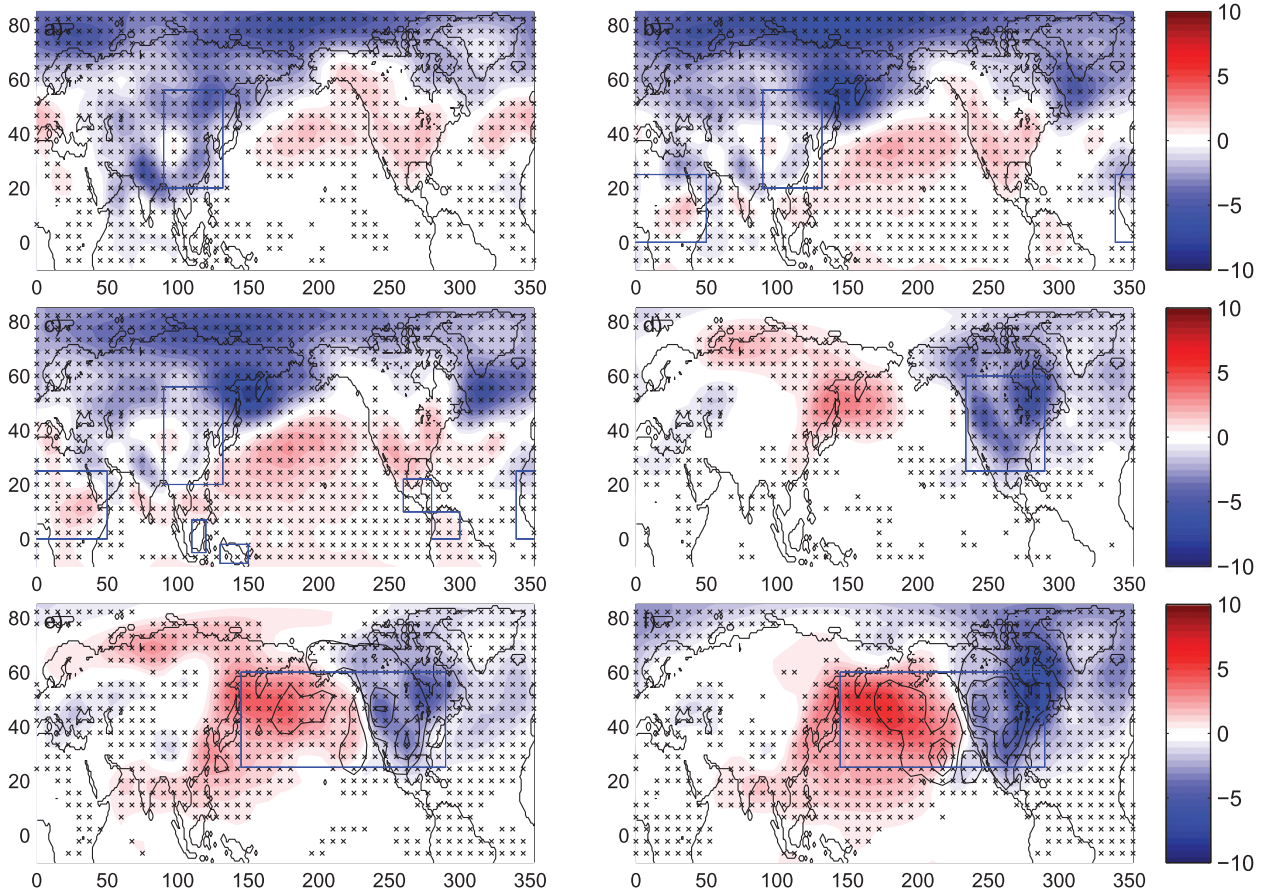


FIG. 7. Surface pressure response (hPa) to changes in the diabatic heating over (a) Southeast Asia; (b) Southeast Asia and North Africa; (c) North Africa, Southeast Asia, Indonesia, and northern South America; and (d) North America. SSOL – WSOL anomalies of SLP (colors) and diabatic heating (contours) at the 0.9 sigma level for (e) LOHC1 and (f) LOHC2 experiments. The intervals for the diabatic heating are  $10^{-5} \text{ K s}^{-1}$  (first contour has value  $0.5 \times 10^{-5} \text{ K s}^{-1}$ ). Blue boxes represent the geographical areas where  $Q_{\text{SSOL}}$  was used. Markers ( $\times$ ) show the statistical significance at the 95% level of significance.

Atlantic exhibit some similarities. This implies that these temperature anomalies are being advected by the mean flow of the basic state (climatological circulation; Fig. 8, bottom left) and that they are not the result of the anticyclonic anomalies.

The advection of the temperature anomalies is related to a reduction of the meridional temperature gradient (Fig. 8, bottom right). The meridional temperature gradient is always related with the baroclinic activity, which is relatively weak in the Northern Hemisphere during JJA. Consequently, the large reduction of the meridional temperature gradient located over the central North Pacific ( $30^{\circ}$ – $55^{\circ}\text{N}$ ) implies that the baroclinic activity in that region gets even weaker, and the SLP increases. The implication of this is that the weakening of the baroclinic activity in the North Pacific contributes to the development of the anticyclonic anomaly in the North Pacific; especially to its poleward extent (evaluating quantitatively this contribution is difficult). This is

consistent with the mechanism proposed by Nigam and Chan (2009), according to which the strength of the subtropical highs in the Northern Hemisphere peaks during the summer because of the weakening and the northward retreat of the baroclinic activity. The weakening of the North Pacific baroclinic activity is also seen in the decrease in the large-scale precipitation that extends over the same region (Fig. 3, middle), which is also associated with a decrease in latent heat release. In the Atlantic region the change in the meridional temperature gradient is smaller and is not reflected as much in the large-scale precipitation change. In contrast, convective precipitation exhibits a basinwide decrease in both North Atlantic and North Pacific (Fig. 3, bottom). This is because the temperature increase in the upper troposphere (200 hPa) is  $2^{\circ}$ – $5^{\circ}\text{C}$  greater than the increase in the lower troposphere (1000 hPa) and causes a stabilization of the atmospheric column (not shown). The reduction in the convective precipitation in the North

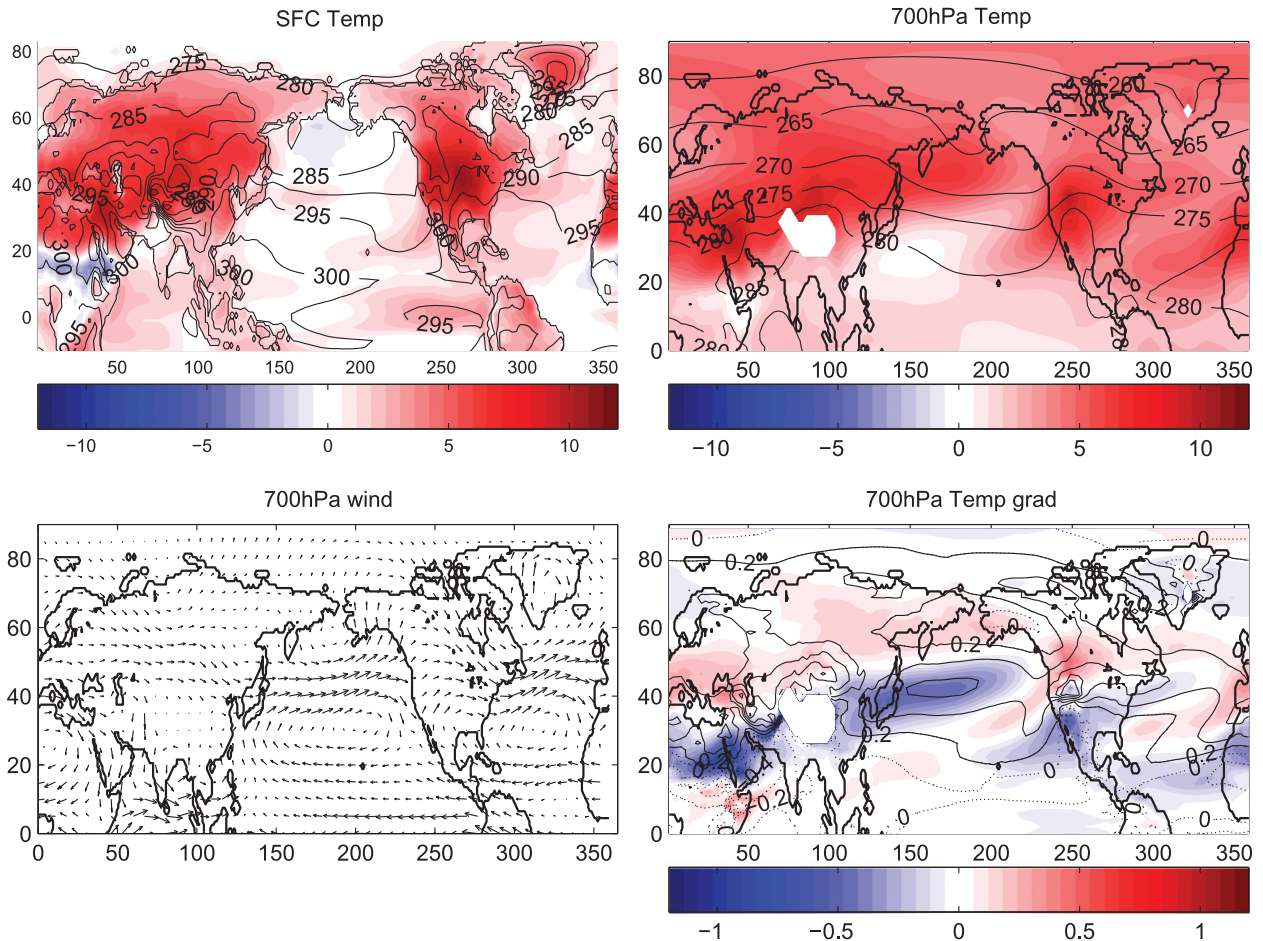


FIG. 8. The JJA conditions for (top) (left) surface temperature and (right) 700-hPa temperature. (bottom) (left) The 700-hPa wind vectors and (right) 700-hPa meridional temperature gradient [ $\text{K} (100 \text{ km})^{-1}$ ]. Contours correspond to climatological values (WSOL climate), and colors correspond to SSOL – WSOL anomalies. Contours for the meridional temperature gradient are every  $0.2 \text{ K} (100 \text{ km})^{-1}$ .

Pacific is basinwide and with a small magnitude, but in the Atlantic it is greater, with maximum values in the western basin.

These changes in precipitation have implications for the existence of the Northern Hemisphere summer anticyclonic anomalies. This is because they are related to the reduction in the latent heat release that make a large fraction of the vertical profile of the change in the total diabatic heating, which acts as local forcing for the anticyclonic anomalies, as seen from the AGCM experiments.

Another large contributor to the vertical profile of the total diabatic heating is the absorption of SW radiation that stems from the increase in the TOA summer insolation and changes in clouds. The JJA low cloud cover increases in both the North Atlantic and North Pacific basins (Fig. 9, top left). This similarity in the low cloud response in both basins is partly responsible for the

similarity between the changes in the vertical profile of the LW part of the diabatic heating in the two basins (Fig. 6, first two panels).

Low clouds are closely related to the stability conditions of the lower troposphere. One measure of stability conditions in the lower troposphere is the estimated inversion strength (EIS) as defined by Wood and Bretherton (2006):

$$\begin{aligned} \text{EIS} &= \text{LTS} - \Gamma_m^{850} (z_{700} - \text{LCL}) \\ &= \theta_{700} - \text{SST} - \Gamma_m^{850} (z_{700} - \text{LCL}), \end{aligned} \quad (1)$$

where  $\theta_{700}$  represents the potential temperature at 700 hPa, SST is the sea surface temperature,  $\Gamma_m^{850}$  is the moist adiabatic lapse rate at 850 hPa,  $z_{700}$  is the height at 700 hPa, and LCL represents the lifting condensation level. An inspection of the changes in EIS reveals that the EIS increases in almost the entire North Pacific and

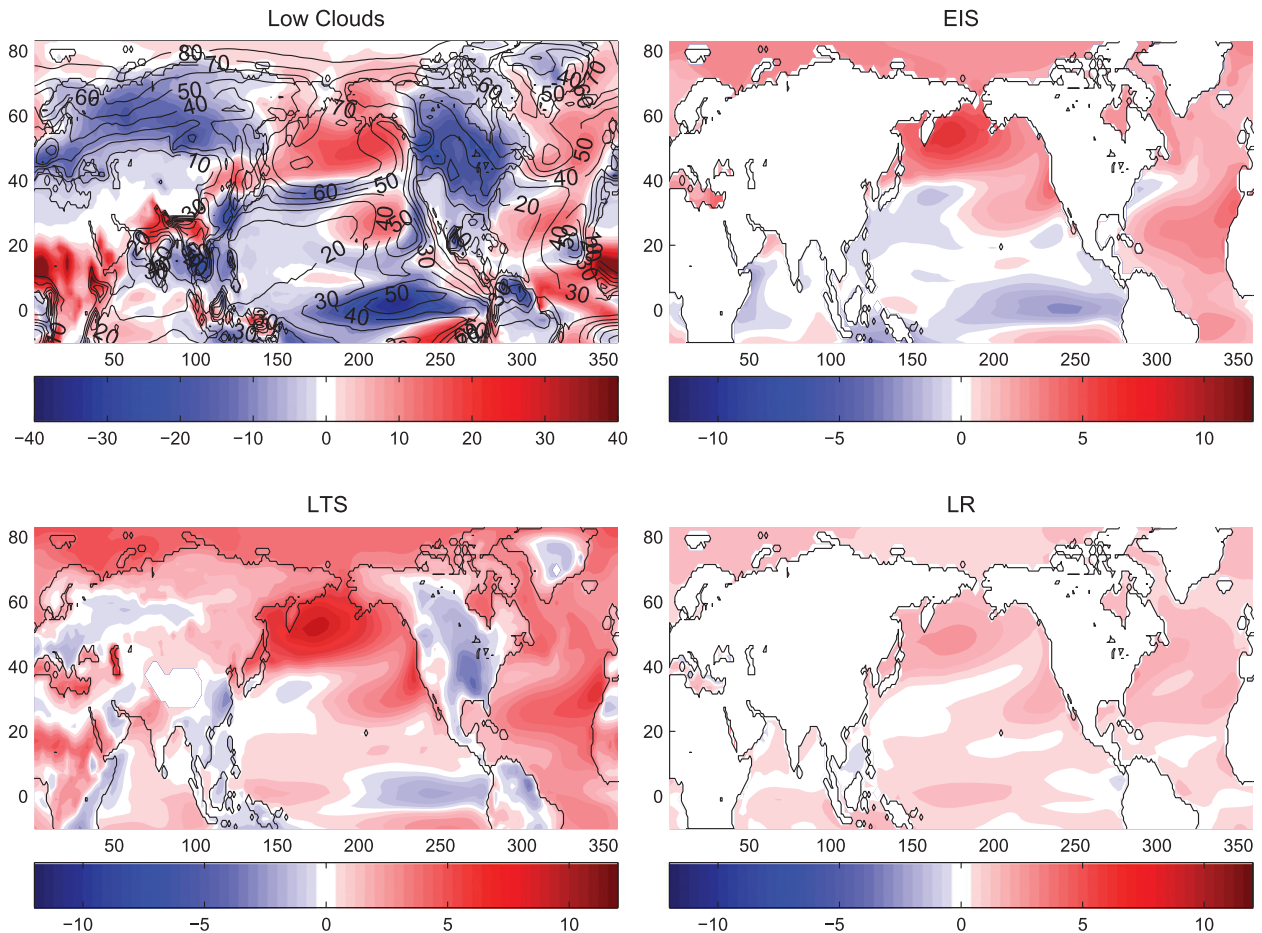


FIG. 9. (a) Climatology (contours) and SSOL – WSOL anomalies (colors) for JJA low cloud distribution. SSOL – WSOL anomalies of (b) EIS, (c) LTS, and (d) LR, (e)  $\theta_{700}$ , and (f) surface temperature ( $^{\circ}\text{C}$ ). The minus sign from Eq. (2) has not been added to the LR term.

North Atlantic basin (Fig. 9, top right), with the maximum values corresponding to regions where low clouds have maximum increase in cloud fraction. However, it should be noted that along the west coast of North America and North Africa, local maxima of positive EIS anomalies do not correspond to an increase in low cloud fraction but actually correspond to a reduction, indicating that other processes must be involved. A separation of the EIS anomalies into anomalies corresponding to the lower tropospheric stability (LTS; Fig. 9, bottom left) and the lapse rate term [ $\text{LR} = \Gamma_m^{850}(z_{700} - \text{LCL})$ ; Fig. 9, bottom right] reveals that the LTS anomalies dominate, with LR having a smaller contribution to the EIS changes. A further separation of the LTS anomalies into anomalies of SST and  $\theta_{700}$  (Fig. 8, top panels) reveals that the increase in  $\theta_{700}$  has the biggest contribution. Generally, the LTS strengthens because the temperature of the free troposphere that caps the boundary layer exhibits a larger increase compared to the surface temperature. Only in the North Pacific does the reduction observed in the SSTs

assist the development of the local LTS maxima. Again, we suggest that the precession-induced continental heating, which extends to higher levels and is being advected by the mean atmospheric circulation over the ocean basins, is partly responsible for the strengthening of the LTS and the low cloud fraction. It is interesting to note the fact that the LR anomalies have a similar spatial variability with the LTS anomalies, which stems from the fact that the LR reflects the change in the moist adiabatic lapse rate due to the heating observed above the boundary layer. The result is that the total diabatic heating in the North Pacific and North Atlantic, associated with the changes in precipitation, cloud cover, and incoming solar radiation, have a similar vertical profile.

## 6. Nonlinear effect and relevance to linear dynamics

Previous studies (Rodwell and Hoskins 2001; Nigam and Chan 2009; Miyasaka and Nakamura 2005, 2010)

have investigated the presence, as well as the twentieth-century variability, of the summer subtropical highs through linear wave dynamics. In contrast, our study uses a nonlinear model and investigates the equilibrated fully nonlinear response. Here we address to what extent the fully nonlinear response is different from the linear response and how relevant are our results with the mechanisms proposed by other studies.

Nigam and Chan (2009) showed that the SLP response to the diabatic heating (climatological values) placed in the Asian monsoon region is a zonally uniform positive anomaly extending from the central North Pacific all the way to the central North Atlantic (Fig. 11a in Nigam and Chan 2009). This is also supported by results from Rodwell and Hoskins (2001) that show that the 887-hPa horizontal streamfunction of the linear response to diabatic heating associated with the Asian summer monsoon is positive in the same region (see Fig. 8b in Rodwell and Hoskins 2001). These are consistent with our fully nonlinear SLP response to changes in the diabatic heating in the Southeast Asian monsoon region (Fig. 7a), even though the diabatic heating is represented by SSOL – WSOL anomalies and not climatological values, and also despite the fact that is placed in a slightly different region.

Additionally, the simulation of the North Pacific circulation response to the change in the local lower tropospheric land–ocean heating contrast (experiments LOCH1 and LOCH2) is consistent with the results of Miyasaka and Nakamura (2005, 2010). These studies showed that the linear response to the lower tropospheric land–ocean heating contrast, due to radiative cooling associated with low clouds over the northeast Pacific and sensible heating over land to the east, can explain a large fraction of the surface North Pacific anticyclone.

The conclusion is that our results suggest that the fully nonlinear response used in this study is generally consistent with the linear wave dynamics theory used in previous studies. It should be noted that this might not be the case in the presence of a stronger zonal circulation like the winter season or the Southern Hemisphere.

## 7. Limitations of this study

It is worth highlighting some of the limitations of this study. First, the primitive equation atmospheric model is run with a coarse resolution:  $7.5^\circ \times 4.5^\circ$  in the horizontal and five sigma levels in the vertical. Even though the imposed  $Q$ , attributed to the ITCZ, monsoons, or storm tracks, is represented horizontally, a higher horizontal resolution might slightly influence the idealized experiments with the AM. On the other hand, the five levels of the vertical resolution are expected to have a higher

impact on the results because they underestimate the vertical distribution (corresponding to CM2.1; Fig. 6) of  $Q$ , especially in the lower boundary. Second, the simulated change in the anticyclones (by CM2.1) depends on how accurate the simulated change of the diabatic heating is. As it turns out, this depends on several processes, like the change in the monsoons and low clouds. For clouds, and especially low cloud types, it is widely known that they provide the biggest uncertainty in model climate sensitivity (Soden and Held 2006; Soden and Vecchi 2011). Therefore, if the model overestimates one or the other, this might also affect the anticyclonic response. Such limitations certainly imply that any interpretation of the results of this study should be done with caution. However, the fact that the idealized experiments with AM reproduce the anticyclonic anomalies simulated by CM2.1 does work in our advantage.

Another question involves the realism of the model's (CM2.1) representation of the anticyclones. According to Delworth et al. (2006), CM2.1 slightly overestimates the strength of the summer subtropical highs [ $\sim(1\text{--}3)$  hPa] in the North Pacific and North Atlantic compared to twentieth-century observations. The representation of precipitation by CM2.1 also has some biases, which are larger in the monsoonal regions and should be taken into account since the monsoons are shown to remotely affect the subtropical highs. All of these biases could affect the simulation of the response of the subtropical highs by CM2.1; however, it is not possible to know to what extent.

## 8. Summary and concluding remarks

The variability of the Northern Hemisphere summer anticyclones due to a change in Earth's precession is investigated using GFDL CM2.1. A change in the location of the perihelion from the winter to the summer solstice of the Northern Hemisphere causes a strengthening and a westward expansion of the Northern Hemisphere summer subtropical highs. The response is stronger over the Pacific than the Atlantic.

Experiments with a primitive equation atmospheric model show that the anticyclonic anomalies stationed over the North Pacific and North Atlantic are both forced locally and remotely by changes in diabatic heating. Changes in the local diabatic heating in the North Atlantic and North Pacific are comparable and partly explain the anomalous anticyclonic circulation stationed over each basin. These changes are related to a reduction in the latent heat release due to a reduction in precipitation. These result from a stabilization of the atmospheric column that suppresses convective activity, as well as a weakening of the baroclinic activity that is

quite pronounced in the Pacific region and suppresses the large-scale precipitation. Changes in local diabatic heating are also related to the increase in low cloud fraction over the North Atlantic and North Pacific that reduces the LW part of the diabatic heating in the lower troposphere and to the increase in absorption of SW radiation by the atmosphere.

Almost half of the anticyclonic anomaly over the northern Pacific is remotely forced by diabatic heating over the neighboring continents. This remote influence can be attributed to a change in the diabatic heating associated with the strengthening of the monsoons, mainly in Southeast Asia, and to a smaller extent in North Africa. Heating over North America also contributes to the development of an anticyclonic response in the northwestern Pacific. For the anticyclonic anomalies over the North Atlantic, changes in the diabatic heating over land have only a small remote influence (for reasons that were not the subject of this study), which is the reason why the anomaly is smaller compared to that stationed over the North Pacific. Remote forcing also comes from the tropical oceans. For example, the weakening of the Atlantic ITCZ has an anticyclonic response over the North Atlantic.

Regarding the mechanisms proposed to explain the strength and existence of the subtropical highs, our study shows that all three mechanisms—1) remote monsoonal effect, 2) effects from the local land–ocean heating contrast of the lower troposphere, and 3) weakening of the baroclinic activity—are relevant and could also be mutually reinforcing each other. Strengthening of the monsoonal activity has a major role in the remote influence of the Pacific anticyclone, and the strengthening of the land–ocean heating contrast between the North Pacific and North America also seems to be important. The weakening of the storm track seems to be consistent with the anticyclonic anomaly in the North Pacific, but its effect is probably weaker compared to the other mechanisms.

We have not addressed the changes in the December–February (DJF) circulation in the Southern Hemisphere. The reason for this is that AM experiments performed with DJF diabatic forcing do not reproduce the full model SLP response (not shown). This implies that the circulation response to changes in the diabatic heating is overwhelmed by internal dynamics (baroclinic instability and nonlinearity). We tested whether stronger coupling of the simulated circulation to the meridional temperature gradient in the lower troposphere could improve the AM simulation of the Southern Hemisphere circulation response (Lindzen and Nigam 1987). To do this, we increased the Newtonian cooling by reducing the time scale parameter from 20 days to 10 and 5 days in the two lower levels (0.7 and 0.9 sigma levels). However, the results (not

shown) indicate that the stronger coupling of the circulation to the meridional temperature gradient did not improve the simulation of the Southern Hemisphere circulation response. Additionally, an attempt to increase the relative effect of the diabatic heating on the circulation by reducing the Newtonian cooling at all vertical levels in the AM also failed to reproduce the SLP changes simulated by the full model. This supports the interpretation that the simulation of Southern Hemisphere summer anticyclones in CM2.1 is more strongly influenced by internal atmospheric dynamics than by diabatic forcing.

Recent studies question whether the variability of  $\delta^{18}\text{O}$  from Southeast Asian caves can be attributed to the precession-induced local insolation changes (LeGrande and Schmidt 2009; Pausata et al. 2011), but our study shows that more precipitation is simulated in Southeast Asia when the longitude of the perihelion is located on the summer solstice. The remote effect the monsoons have on the North Pacific summer anticyclone also has implications for the interpretation of local ocean proxies. Temperature proxies are more likely to reflect the changes attributed to the wind field (affecting ocean advection and upwelling) and not changes in local insolation. On the other hand, precipitation proxies over the northern oceans would reflect a general weakening and not a shift, as is often the case in the tropics.

*Acknowledgments.* This work was supported by an NSF Paleoclimate program, Grant ATM0902926. Damianos F. Mantsis acknowledges partial support from the National Science Fund (NSF) Paleoclimate Perspectives on Climate Change Initiative Grant AGS-1103209 (Ben R. Lintner, PI).

## REFERENCES

- Bourke, W., 1974: A multi-level spectral model. I. Formulation and hemispheric integrations. *Mon. Wea. Rev.*, **102**, 687–701.
- Braconnot, P., S. Joussaume, O. Marti, and N. de Noblet, 1999: Synergistic feedbacks from ocean and vegetation on the African monsoon response to mid-Holocene insolation. *Geophys. Res. Lett.*, **26**, 2481–2484.
- , and Coauthors, 2007a: Results of PMIP2 coupled simulations of the mid-Holocene and last glacial maximum—Part I: Experiments and large-scale features. *Climate Past*, **3**, 261–277.
- , and Coauthors, 2007b: Results of PMIP2 coupled simulations of the mid-Holocene and last glacial maximum—Part II: Feedbacks with emphasis on the location of the ITCZ and mid- and high-latitudes heat budget. *Climate Past*, **3**, 279–296.
- Chen, P., M. P. Hoerling, and R. M. Dole, 2001: The origin of the subtropical anticyclones. *J. Atmos. Sci.*, **58**, 1827–1835.
- Clement, A. C., A. Hall, and A. J. Broccoli, 2004: The importance of precessional signals in the tropical climate. *Climate Dyn.*, **22**, 327–341.

- Coe, M. T., and S. P. Harrison, 2002: The water balance of northern Africa during the mid-Holocene: An evaluation of the 6ka BP PMIP simulations. *Climate Dyn.*, **19**, 155–166.
- Delworth, T. L., and Coauthors, 2006: GFDL's CM2 global coupled climate models. Part I: Formulation and simulation characteristics. *J. Climate*, **19**, 643–674.
- Fleitmann, D., and Coauthors, 2006: Holocene ITCZ and Indian monsoon dynamics recorded in stalagmites from Oman and Yemen (Socotra). *Quat. Sci. Rev.*, **26**, 170–188.
- Hoskins, B., 1996: On the existence and strength of the summer subtropical anticyclones. *Bull. Amer. Meteor. Soc.*, **77**, 1287–1291.
- Hsu, Y.-H., C. Chou, and K.-Y. Wei, 2010: Land–ocean asymmetry of tropical precipitation changes in the mid-Holocene. *J. Climate*, **23**, 4133–4151.
- Jolly, D., and Coauthors, 1998: Biome reconstruction from pollen and plant macrofossil data for Africa and the Arabian Peninsula at 0 and 6 ka. *J. Biogeogr.*, **25**, 1007–1027.
- Joussaume, S., and P. Braconnot, 1997: Sensitivity of paleoclimate simulation results to season definitions. *J. Geophys. Res.*, **102**, 1943–1956.
- , and Coauthors, 1999: Monsoon changes for 6000 years ago: Results of 18 simulations from the Paleoclimate Modeling Intercomparison Project (PMIP). *Geophys. Res. Lett.*, **26**, 859–862.
- Kirtman, B. P., D. A. Paolino, J. L. Kinter III, and D. M. Straus, 2001: Impact of tropical subseasonal SST variability on seasonal mean climate. *Mon. Wea. Rev.*, **129**, 853–868.
- Kutzbach, J. E., 1981: Monsoon climate of the early Holocene: Climate experiment with the earth's orbital parameters for 9000 years ago. *Science*, **214**, 59–61.
- , and Z. Liu, 1997: Response of the African monsoon to orbital forcing and ocean feedbacks in the middle Holocene. *Science*, **278**, 440–443.
- LeGrande, A. N., and G. A. Schmidt, 2009: Sources of Holocene variability of oxygen isotope paleoclimate archives. *Climate Past*, **5**, 441–455.
- Lezine, A.-M., W. Zheng, P. Braconnot, and G. Krinner, 2011: Late Holocene plant and climate evolution at Lake Yoa, northern Chad: Pollen data and climate simulations. *Climate Past*, **7**, 1351–1362.
- Li, W., L. Li, R. Fu, Y. Deng, and H. Wang, 2011: Changes to the North Atlantic subtropical high and its role in the intensification of summer rainfall variability in the southeastern United States. *J. Climate*, **24**, 1499–1506.
- Lindzen, R. S., and S. Nigam, 1987: On the role of sea surface temperature gradient in forcing low-level winds and convergence in the tropics. *J. Atmos. Sci.*, **44**, 2418–2436.
- Marzin, C., and P. Braconnot, 2009: Variations of Indian and African monsoons induced by insolation changes at 6 and 9.5 kyr BP. *Climate Past*, **33**, 215–231.
- Miyasaka, T., and H. Nakamura, 2005: Structure and formation mechanisms of the Northern Hemisphere summertime subtropical highs. *J. Climate*, **18**, 5046–5065.
- , and —, 2010: Structure and mechanisms of the Southern Hemisphere summertime subtropical anticyclones. *J. Climate*, **23**, 2115–2130.
- Nigam, S., and S. C. Chan, 2009: On the summertime strengthening of the Northern Hemisphere Pacific sea level pressure anticyclone. *J. Climate*, **22**, 1174–1192.
- Partridge, C. T., P. B. DeMenocal, S. A. Lorentz, M. J. Paiker, and J. C. Vogel, 1997: Orbital forcing of climate over South Africa: A 200,000-year rainfall record from the Pretoria saltpan. *Quat. Sci. Rev.*, **16**, 1125–1133.
- Pausata, F. S. R., D. S. Battisti, K. H. Nisancioglu, and C. M. Bitz, 2011: Chinese stalagmite  $\delta^{18}\text{O}$  controlled by changes in the Indian monsoon during a simulated Heinrich event. *Nat. Geosci.*, **4**, 474–480.
- Pollard, D., and D. B. Reusch, 2002: A calendar conversion method for monthly mean paleoclimate model output with orbital forcing. *J. Geophys. Res.*, **107**, 4615, doi:10.1029/2002JD002126.
- Prell, W. L., and J. E. Kutzbach, 1992: Sensitivity of the Indian monsoon to forcing parameters and implications for its evolution. *Nature*, **360**, 647–652.
- Rodwell, M. J., and B. J. Hoskins, 2001: Subtropical anticyclones and summer monsoons. *J. Climate*, **14**, 3192–3211.
- Seager, R., R. Murtugudde, N. Naik, A. Clement, N. Gordon, and J. Miller, 2003: Air–sea interaction and the seasonal cycle of the subtropical anticyclones. *J. Climate*, **16**, 1948–1966.
- Soden, J. B., and I. M. Held, 2006: An assessment of climate feedbacks in coupled ocean–atmosphere models. *J. Climate*, **19**, 3354–3360.
- , and G. A. Vecchi, 2011: The vertical distribution of cloud feedback in coupled ocean–atmosphere models. *Geophys. Res. Lett.*, **38**, L12704, doi:10.1029/2011GL047632.
- Vernekar, A. D., J. Zhou, and B. P. Kirtman, 1992: Comparison of systematic errors in two forecast models with similar dynamical frameworks. *Atmósfera*, **5**, 207–231.
- Wang, Y., and Coauthors, 2008: Millennial- and orbital-scale changes in the East Asian monsoon over the past 224,000 years. *Nature*, **451**, 1090–1093.
- Wood, R., and C. S. Bretherton, 2006: On the relationship between stratiform low cloud cover and lower tropospheric stability. *J. Climate*, **19**, 6425–6432.
- Wu, G., and Y. Liu, 2003: Summertime quadruplet heating pattern in the subtropics and the associated atmospheric circulation. *Geophys. Res. Lett.*, **30**, 1201, doi:10.1029/2002GL016209.
- Wu, H., J. Guiot, S. Brewer, and Z. Guo, 2007: Climatic changes in Eurasia and Africa at the last glacial maximum and mid-Holocene: Reconstruction from pollen data using inverse vegetation modeling. *Climate Dyn.*, **29**, 211–229.
- Zhou, T., and Coauthors, 2009: Why the western Pacific subtropical high has extended westward since the late 1970s. *J. Climate*, **22**, 2199–2215.